

Purely Quantum Nonreciprocity by Spatially Separated Transmission Scheme

Zhi-Hao Liu,¹ Guang-Yu Zhang,¹ and Xun-Wei Xu^{1,2,*}

¹*Key Laboratory of Low-Dimensional Quantum Structures and Quantum Control of Ministry of Education, Key Laboratory for Matter Microstructure and Function of Hunan Province, Department of Physics and Synergetic Innovation Center for Quantum Effects and Applications, Hunan Normal University, Changsha 410081, China*

²*Institute of Interdisciplinary Studies, Hunan Normal University, Changsha, 410081, China*

(Dated: June 11, 2024)

Nonreciprocal photon blockade is of particular interest due to its potential applications in chiral quantum technologies and topological photonics. In the regular cases, nonreciprocal transmission (classical nonreciprocity) and nonreciprocal photon blockade (quantum nonreciprocity) often appear simultaneously. Nevertheless, how to achieve *purely* quantum nonreciprocity (no classical nonreciprocity) remains largely unexplored. Here, we propose a spatially separated transmission scheme, that the photons transport in different directions take different paths, in an optical system consisting of two spinning cavities coupled indirectly by two common drop-filter waveguides. Based on the spatially separated transmission scheme, we demonstrate a purely quantum nonreciprocity (nonreciprocal photon blockade) by considering the Kerr nonlinear interaction in one of the paths. Interestingly, we find that the nonreciprocal photon blockade is *enhanced nonreciprocally*, i.e., the nonreciprocal photon blockade is enhanced when the photons transport in one direction but suppressed in the reverse direction. We identify that the nonreciprocal enhancement of nonreciprocal photon blockade is induced by the destructive or constructive interference between two paths for two photons passing through the whole system. The spatially separated transmission scheme proposed in the work provides a novel approach to observe purely quantum nonreciprocal effects.

I. INTRODUCTION

Optical nonreciprocal transmission is an interesting phenomenon that photons are allowed to pass in one direction but blocked in the opposite direction. It is pivotal for realizing unidirectional optical devices, including optical isolators [1–6], circulators [7–11], directional amplifiers [12–20], unidirectional frequency converter [21–27], etc. By breaking Lorentz reciprocity [28], optical nonreciprocity has been observed based on the magneto-optic effect [29–31], optical nonlinearity [32–34], synthetic magnetism [35–38], indirect interband transition [39–42], parity-time symmetry breaking [43–46], Doppler effect [47–50], chiral interaction [51–53], and so on.

As an important development direction, the concept of optical nonreciprocity was extended from the classical regime to quantum regime, and various of quantum nonreciprocal effects were predicted, e.g., nonreciprocal photon blockade [54–58], nonreciprocal entanglement [59–62], and nonreciprocal squeezing [63–66]. For example, nonreciprocal photon blockade is referred to the phenomenon that photon blockade happens when the cavity is driven in one direction but not the other, which opens a route for chiral quantum manipulation of light. In a recent work, chiral cavity quantum electrodynamics system is experimentally demonstrated with multiple atoms strongly coupled to a Fabry–Pérot cavity [67].

Different from classical nonreciprocity, nonlinear interaction is an essential prerequisite to nonreciprocally

manipulate the quantum properties of photons. One of the most popular approaches for quantum nonreciprocity is to introduce nonlinear interactions in the classically nonreciprocal systems, such as spinning resonators with additional Kerr nonlinearity [54, 68], second-order nonlinearity [69–71], optomechanical interaction [72–74], or atom-cavity interaction [75–79]. In such cases, nonreciprocal transmission (classical nonreciprocity) and nonreciprocal photon blockade (quantum nonreciprocity) often appear simultaneously. Here, we consider another interesting quantum nonreciprocity that nonreciprocal photon blockade is achieved without classical nonreciprocity, referred to as *purely* quantum nonreciprocity. Except for a few exceptions [80–82], purely quantum nonreciprocity is hard to achieve based on the popular approaches for quantum nonreciprocity, because the paths for the photon transmission are spatially unseparated, i.e., the photons travel in opposite directions but in the same resonator (path).

In this paper, we propose a spatially separated transmission scheme to achieve purely quantum nonreciprocity, in an optical system consisting of two spinning cavities coupled indirectly by two common drop-filter waveguides. We show that the photons transport between two ports with the same transmission rate (classical nonreciprocity), but photons pass through different paths (cavities) when they transport in different directions. Due to the Kerr nonlinear interaction in one of the paths, we demonstrate nonreciprocal photon blockade (purely quantum nonreciprocity) via the spatially separated transmission scheme. Surprisingly, we find that the nonreciprocal photon blockade is enhanced nonreciprocally, i.e., the nonreciprocal photon blockade is en-

* xwxu@hunnu.edu.cn

hanced when the photons transport in one direction but suppressed in the reverse direction. We identify that the nonreciprocal enhancement of nonreciprocal photon blockade is induced by the destructive or constructive interference between two paths for two photons passing through the whole system. Spatially separated transmission scheme provides a novel approach for purely quantum nonreciprocity.

This paper is organized as follows: In Sec. II, we introduce a physical model consisting of a spinning Kerr cavity and a spinning linear cavity coupled indirectly by two common drop-filter waveguides. In Sec. III, we explore the spatially separated transmission scheme and show the paths of the photons when they transport in different directions. In Sec. IV, we demonstrate the nonreciprocal photon blockade and its nonreciprocal enhancement effect based on numerical simulations. The mechanism for the nonreciprocal enhancement of nonreciprocal photon blockade is analyzed analytically in Sec. V. Finally, a conclusion is given in Sec. VI.

II. PHYSICAL MODEL

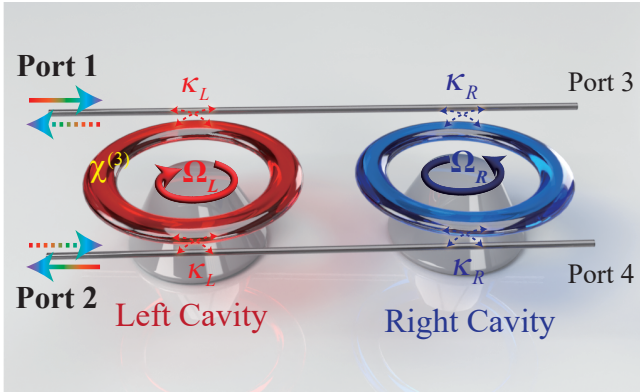


FIG. 1. The schematic diagram of the optical system: A spinning nonlinear optical cavity (left) and a spinning linear optical cavity (right) are coupled to two common drop-filter waveguides (four ports) with coupling strengths (decay rates κ_L and κ_R), and a weak driving field (frequency ω_d) is input from Port 1 or Port 2.

The optical system we consider is illustrated in Fig. 1. A spinning nonlinear optical cavity (left) and a spinning linear optical cavity (right) are coupled to two common drop-filter waveguides (four ports) with coupling strengths (decay rates κ_L and κ_R), and a weak driving field (frequency ω_d) is input from Port 1 or Port 2. In a frame rotating at the driving frequency ω_d , the system can be described by the Hamiltonian ($\hbar = 1$)

$$\begin{aligned}
 H_\sigma = & \Delta_{L,\sigma} a_{L,\sigma}^\dagger a_{L,\sigma} + U a_{L,\sigma}^\dagger a_{L,\sigma}^\dagger a_{L,\sigma} a_{L,\sigma} \\
 & + \Delta_{R,\sigma} a_{R,\sigma}^\dagger a_{R,\sigma} + J_{\text{eff}} (a_{L,\sigma}^\dagger a_{R,\sigma} + a_{R,\sigma}^\dagger a_{L,\sigma}) \\
 & + i(\varepsilon_L a_{L,\sigma}^\dagger - \varepsilon_R e^{i\theta} a_{R,\sigma}^\dagger - \text{H.c.}), \quad (1)
 \end{aligned}$$

where $\sigma = \text{cw}$ corresponds to the case that the weak driving field is input from Port 1, and the clockwise modes ($a_{L,\text{cw}}$ and $a_{R,\text{cw}}$) are excited; $\sigma = \text{ccw}$ corresponds to the case that the weak driving field is input from Port 2, and the counter-clockwise modes ($a_{L,\text{ccw}}$ and $a_{R,\text{ccw}}$) are excited. ω_L (ω_R) is the resonance frequency of the left (right) cavity without spinning. The detunings are given by $\Delta_{L,\text{cw}} = \Delta_L - \Delta_{F,L}$, $\Delta_{L,\text{ccw}} = \Delta_L + \Delta_{F,L}$, $\Delta_{R,\text{cw}} = \Delta_R + \Delta_{F,R}$, $\Delta_{R,\text{ccw}} = \Delta_R - \Delta_{F,R}$, $\Delta_L = \omega_L - \omega_d$ and $\Delta_R = \omega_R - \omega_d$. Here, we consider the case that the left (right) cavity rotates clockwise (counterclockwise) with an angular velocity Ω_L (Ω_R), so the left (right) cavity experiences a Fizeau shift $\Delta_{F,L}$ ($\Delta_{F,R}$), with [83]

$$\Delta_{F,j} = \frac{n_j r_j \Omega_j \omega_j}{c} \left(1 - \frac{1}{n_j^2} - \frac{\lambda}{n_j} \frac{dn_j}{d\lambda} \right), \quad (2)$$

where n_j ($j = L, R$) is the refractive index, r_j is the resonator radius of the cavity, λ is the wavelength of the light in vacuum, c is the speed of light in vacuum. The dispersion term $dn/d\lambda$ is originated from the relativistic effect and it is remarkably small (to $\sim 1\%$) [50, 83]. $U = \hbar \omega_L^2 c n_2 / (n_L^2 V_{\text{eff}})$ is the Kerr interaction strength [84], where n_2 is the nonlinear refraction index, and V_{eff} is the effective mode volume. $\varepsilon_L = \sqrt{\kappa_L P_{\text{in}}} / (\hbar \omega_d)$ ($\varepsilon_R = \sqrt{\kappa_R P_{\text{in}}} / (\hbar \omega_d)$) is the driving amplitude of the left (right) cavity, and P_{in} is the driving power. $J_{\text{eff}} = i\sqrt{\kappa_L \kappa_R} e^{i\theta}$ describes the waveguide-induced indirect coupling strength between the two cavities [85], and θ is accumulated phase of light propagating from one cavity to another in the waveguides. Here, we consider $\theta = \pi/2$ so that the Hamiltonian (1) is a Hermitian.

In order to describe the transmission behaviors and quantum statistical properties for the photons transport from Port i to Port j , we define the optical transmission rate T_{ji} and the equal-time second-order correlation function $g_{ji}^{(2)}(0)$ as

$$T_{ji} = \frac{\langle a_{j,\text{out}}^\dagger a_{j,\text{out}} \rangle}{\langle a_{i,\text{in}}^\dagger a_{i,\text{in}} \rangle}, \quad (3)$$

and

$$g_{ji}^{(2)}(0) = \frac{\langle a_{j,\text{out}}^\dagger a_{j,\text{out}}^\dagger a_{j,\text{out}} a_{j,\text{out}} \rangle}{\langle a_{j,\text{out}}^\dagger a_{j,\text{out}} \rangle^2}, \quad (4)$$

where $a_{i,\text{in}}$ is the optical field input from Port i and $a_{j,\text{out}}$ is the optical field output from Port j . In this paper, we focus on the nonreciprocal transmission between Port 1 and 2, with a weak driving field input from Port 1 or Port 2. According to the input-output relations [86], the output fields from Port 1 and 2 ($a_{1,\text{out}}$ and $a_{2,\text{out}}$) can be expressed as

$$a_{1,\text{out}} = \sqrt{\kappa_L} a_{L,\text{ccw}} - i\sqrt{\kappa_R} a_{R,\text{ccw}} + ia_{3,\text{in}}, \quad (5)$$

$$a_{2,\text{out}} = \sqrt{\kappa_L} a_{L,\text{cw}} - i\sqrt{\kappa_R} a_{R,\text{cw}} + ia_{4,\text{in}}, \quad (6)$$

where $a_{3,\text{in}}$ ($a_{4,\text{in}}$) is the input field from Port 3 (Port 4). Here, both $a_{3,\text{in}}$ and $a_{4,\text{in}}$ are vacuum fields.

Specifically, if a coherent field is input from Port 1, i.e., $\langle a_{1,\text{in}} \rangle = \sqrt{P_{\text{in}}}/(\hbar\omega_d)$ and $\langle a_{2,\text{in}} \rangle = 0$, then the transmission rate from Port 1 to 2 is given by

$$T_{21} = T_{21}^L + T_{21}^R + T_{21}^I, \quad (7)$$

where

$$T_{21}^L = \frac{\kappa_L \langle a_{L,\text{cw}}^\dagger a_{L,\text{cw}} \rangle}{\langle a_{1,\text{in}}^\dagger a_{1,\text{in}} \rangle} \quad (8)$$

corresponds to the photons passing through the left cavity,

$$T_{21}^R = \frac{\kappa_R \langle a_{R,\text{cw}}^\dagger a_{R,\text{cw}} \rangle}{\langle a_{1,\text{in}}^\dagger a_{1,\text{in}} \rangle} \quad (9)$$

corresponds to the photons passing through the right cavity, and

$$T_{21}^I = \frac{-2\sqrt{\kappa_L\kappa_R}\text{Re} \left[i \langle a_{L,\text{cw}}^\dagger a_{R,\text{cw}} \rangle \right]}{\langle a_{1,\text{in}}^\dagger a_{1,\text{in}} \rangle} \quad (10)$$

is the interference term between the two paths. In the meantime, the equal-time second-order correlation function $g_{21}^{(2)}(0)$ is given by

$$\begin{aligned} g_{21}^{(2)}(0) = & \frac{1}{\langle a_{2,\text{out}}^\dagger a_{2,\text{out}} \rangle^2} \left(\kappa_L^2 \langle a_{L,\text{cw}}^\dagger a_{L,\text{cw}}^\dagger a_{L,\text{cw}} a_{L,\text{cw}} \rangle \right. \\ & + \kappa_R^2 \langle a_{R,\text{cw}}^\dagger a_{R,\text{cw}}^\dagger a_{R,\text{cw}} a_{R,\text{cw}} \rangle \\ & + 4\kappa_L\kappa_R \langle a_{L,\text{cw}}^\dagger a_{R,\text{cw}}^\dagger a_{L,\text{cw}} a_{R,\text{cw}} \rangle \\ & - 4\kappa_L\sqrt{\kappa_L\kappa_R} \text{Re} \left[i \langle a_{L,\text{cw}}^\dagger a_{L,\text{cw}}^\dagger a_{L,\text{cw}} a_{R,\text{cw}} \rangle \right] \\ & - 4\kappa_R\sqrt{\kappa_L\kappa_R} \text{Re} \left[i \langle a_{L,\text{cw}}^\dagger a_{R,\text{cw}}^\dagger a_{R,\text{cw}} a_{R,\text{cw}} \rangle \right] \\ & \left. - 2\kappa_L\kappa_R \text{Re} \left[\langle a_{L,\text{cw}}^\dagger a_{L,\text{cw}}^\dagger a_{R,\text{cw}} a_{R,\text{cw}} \rangle \right] \right), \quad (11) \end{aligned}$$

which indicates that $g_{21}^{(2)}(0)$ not only relates to the self-correlation of the photons in the two cavities (the first two terms), but also depends on the cross-correlation of the photons between the two cavities (the last four terms).

Similarly, if a coherent field is input from Port 2, i.e. $\langle a_{2,\text{in}} \rangle = \sqrt{P_{\text{in}}}/(\hbar\omega_d)$ and $\langle a_{1,\text{in}} \rangle = 0$, then the transmission rate from Port 2 to 1 is given by

$$T_{12} = T_{12}^L + T_{12}^R + T_{12}^I, \quad (12)$$

with

$$T_{12}^L = \frac{\kappa_L \langle a_{L,\text{ccw}}^\dagger a_{L,\text{ccw}} \rangle}{\langle a_{2,\text{in}}^\dagger a_{2,\text{in}} \rangle} \quad (13)$$

for photons passing through the left cavity,

$$T_{12}^R = \frac{\kappa_R \langle a_{R,\text{ccw}}^\dagger a_{R,\text{ccw}} \rangle}{\langle a_{2,\text{in}}^\dagger a_{2,\text{in}} \rangle} \quad (14)$$

for photons passing through the right cavity, and

$$T_{12}^I = \frac{-2\sqrt{\kappa_L\kappa_R}\text{Re} \left[i \langle a_{L,\text{ccw}}^\dagger a_{R,\text{ccw}} \rangle \right]}{\langle a_{2,\text{in}}^\dagger a_{2,\text{in}} \rangle} \quad (15)$$

for the interference between the two paths. In the meantime, we have the equal-time second-order correlation function

$$\begin{aligned} g_{12}^{(2)}(0) = & \frac{1}{\langle a_{1,\text{out}}^\dagger a_{1,\text{out}} \rangle^2} \left(\kappa_L^2 \langle a_{L,\text{ccw}}^\dagger a_{L,\text{ccw}}^\dagger a_{L,\text{ccw}} a_{L,\text{ccw}} \rangle \right. \\ & + \kappa_R^2 \langle a_{R,\text{ccw}}^\dagger a_{R,\text{ccw}}^\dagger a_{R,\text{ccw}} a_{R,\text{ccw}} \rangle \\ & + 4\kappa_L\kappa_R \langle a_{L,\text{ccw}}^\dagger a_{R,\text{ccw}}^\dagger a_{L,\text{ccw}} a_{R,\text{ccw}} \rangle \\ & - 4\kappa_L\sqrt{\kappa_L\kappa_R} \text{Re} \left[i \langle a_{L,\text{ccw}}^\dagger a_{L,\text{ccw}}^\dagger a_{L,\text{ccw}} a_{R,\text{ccw}} \rangle \right] \\ & - 4\kappa_R\sqrt{\kappa_L\kappa_R} \text{Re} \left[i \langle a_{L,\text{ccw}}^\dagger a_{R,\text{ccw}}^\dagger a_{R,\text{ccw}} a_{R,\text{ccw}} \rangle \right] \\ & \left. - 2\kappa_L\kappa_R \text{Re} \left[\langle a_{L,\text{ccw}}^\dagger a_{L,\text{ccw}}^\dagger a_{R,\text{ccw}} a_{R,\text{ccw}} \rangle \right] \right), \quad (16) \end{aligned}$$

which is used to describe the statistical properties of the photons transport from Port 2 to 1.

The quantum dynamics of the system is governed by the master equation [87]

$$\dot{\rho}_\sigma = -i[H_\sigma, \rho_\sigma] + 2\kappa_1 L[a_{L,\sigma}] \rho_\sigma + 2\kappa_2 L[a_{R,\sigma}] \rho_\sigma, \quad (17)$$

where ρ_σ ($\sigma = \text{cw}, \text{ccw}$) is the density operator and $L[o]\rho_\sigma = o\rho_\sigma o^\dagger - (o^\dagger o \rho_\sigma + \rho_\sigma o^\dagger o)/2$ denotes a Lindblad term for an operator o . The transmission rates and second-order correlation functions can be obtained by solving the master equation numerically.

In this paper, we choose the experimentally accessible parameters as [88–95]: $\lambda_L = \lambda_R = 1550$ nm, $Q_L = Q_R = 2.5 \times 10^9$, $V_{\text{eff}} = 147 \mu\text{m}^3$, $n_2 = 3 \times 10^{-14} \text{ m}^2/\text{W}$, $r_L = r_R = 30 \mu\text{m}$, $n_L = n_R = 1.4$, $P_{\text{in}} = 0.2$ fW, $\Omega_L/2\pi = \Omega_R/2\pi = 9.4$ kHz. For simplicity, we set $\Delta_L = \Delta_R = \Delta$ and $\kappa_L = \kappa_R = \kappa$. In the microring resonators, Q is usually $10^9 - 10^{12}$ [88–90], and V_{eff} is typically $10^2 - 10^4 \mu\text{m}^3$ [93, 94]. The Kerr coefficient can be $n_2 \sim 10^{-14}$ for materials with potassium titanyl phosphate [95]. In addition, the left (right) cavity rotates clockwise (counterclockwise) with frequency $\Omega_L/2\pi = 9.4$ kHz ($\Omega_R/2\pi = 9.4$ kHz), leading to the Fizeau shifts of $\Delta_{F,L} = \Delta_{F,R} = \Delta_F \approx 20\kappa$. The resonator with a radius of 1.1 mm can rotate at an rotation frequency of 6.6 kHz [50], and a higher angular frequency can be achieved for a smaller object, such as the single 100 nm particles with a rotation frequency of GHz has been observed experimentally [96, 97].

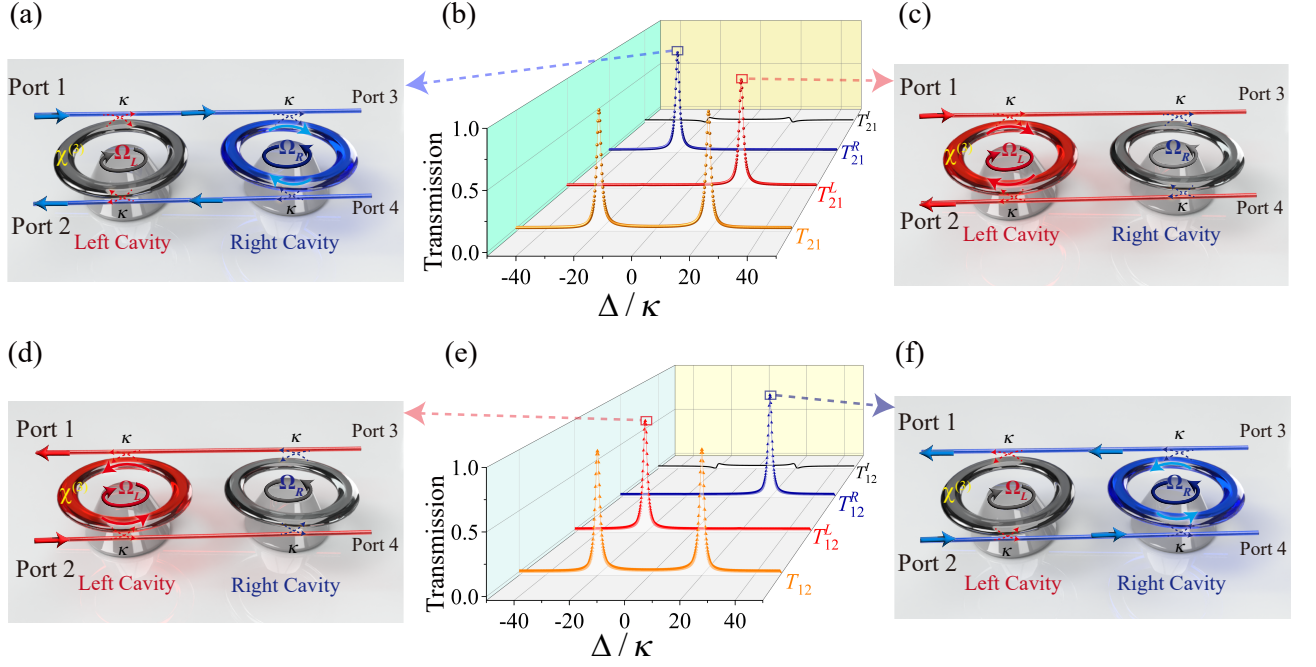


FIG. 2. Spatially separated transmission scheme. (b) The transmission rates T_{21} , T_{21}^L , T_{21}^R , and T_{21}^I versus the detuning Δ/κ ; (e) the transmission rates T_{12} , T_{12}^L , T_{12}^R , and T_{12}^I versus the detuning Δ/κ . (a) and (c) The schematic diagram of the paths for photons transport from Port 1 to 2; (d) and (f) The schematic diagram of the paths for photons transport from Port 2 to 1.

III. SPATIALLY SEPARATED TRANSMISSION

In this section, we introduce a spatially separated transmission scheme that the photons transport from Port 1 to 2 and the ones transport from Port 2 to 1 take different paths (cavities). Under the conditions that the two spatially separated cavities work on the same resonance frequency ($\omega_L = \omega_R$) and they spin in opposite directions with the same rotating frequency ($\Omega_L = \Omega_R$), we find that the photon transmission between Port 1 and 2 is reciprocal, i.e., the transmission rate for photons transport from Port 1 to 2 is the same as the one for photons transport from Port 2 to 1 ($T_{21} \approx T_{12}$) in the whole spectra, as shown in Figs. 2(b) and 2(e). However, the photons input from different ports take different paths (cavities), which is the ingredient for purely quantum nonreciprocity (no classical nonreciprocity) we will discuss in the next section.

According to Eq. (7), the transmission spectrum for the photons transport from Port 1 to 2 can be divided into three parts: T_{21}^L , T_{21}^R , and T_{21}^I , as shown in Fig. 2(b). There are two resonance peaks in the transmission spectra T_{21} , i.e., $\Delta \approx \pm 20\kappa$. The resonance transmission around the detuning $\Delta = 20\kappa$ corresponds to the case that the photons transport from Port 1 to 2 by passing through the left cavity with $T_{21}^L \approx 1$ [Fig. 2(c)]. In contrast, resonance transmission around the detuning $\Delta = -20\kappa$ corresponds to the case that photons transport from Port 1 to 2 by passing through the right cavity with $T_{21}^R \approx 1$ [Fig. 2(a)]. Moreover, the interference

term T_{21}^I is very small and can be ignored, due to the large detuning between the resonance frequencies for the two optical cavities spinning in the opposite direction, $|\Delta_{L,cw} - \Delta_{R,cw}| \approx 40\kappa$.

The transmission spectrum for the photons transport from Port 2 to 1 can also be divided into three parts [Eq. (12)]: T_{12}^L , T_{12}^R , and T_{12}^I , as shown in Fig. 2(e). There are also two resonance peaks in the transmission spectra T_{12} , i.e., $\Delta \approx \pm 20\kappa$. Different from the case of the photons transport from Port 1 to 2, the resonance transmission around the detuning $\Delta = 20\kappa$ corresponds to the case that the photons transport from Port 2 to 1 by passing through the right cavity with $T_{12}^R \approx 1$ [Fig. 2(f)]. In contrast, resonance transmission around the detuning $\Delta = -20\kappa$ corresponds to the case that photons transport from Port 2 to 1 by passing through the left cavity with $T_{12}^L \approx 1$ [Fig. 2(d)]. The interference term T_{12}^I is also very small and can be ignored due to the large detuning between the resonance frequencies for the two optical cavities spinning in the opposite direction.

Based on the above discussion, we have confirmed that the photon transmission between Port 1 and 2 is reciprocal, i.e., $T_{21} \approx T_{12}$, but the photons pass through different paths when they transport in different directions. To be more specific, at detuning $\Delta \approx 20\kappa$, the photons transport from Port 1 to 2 by passing through the left cavity with $T_{21}^L \approx 1$, while the photons transport from Port 2 to 1 by passing through the right cavity with $T_{12}^R \approx 1$; in contrast, at detuning $\Delta \approx -20\kappa$, the photons transport from Port 1 to 2 by passing through the right cavity with

$T_{21}^R \approx 1$, while the photons transport from Port 2 to 1 by passing through the left cavity with $T_{12}^L \approx 1$. Such a spatially separated transmission scheme provides us an ideal platform to realize purely quantum nonreciprocity (no classical nonreciprocity) by considering the nonlinear interaction in one of the paths (cavities).

IV. PURELY QUANTUM NONRECIPROCITY

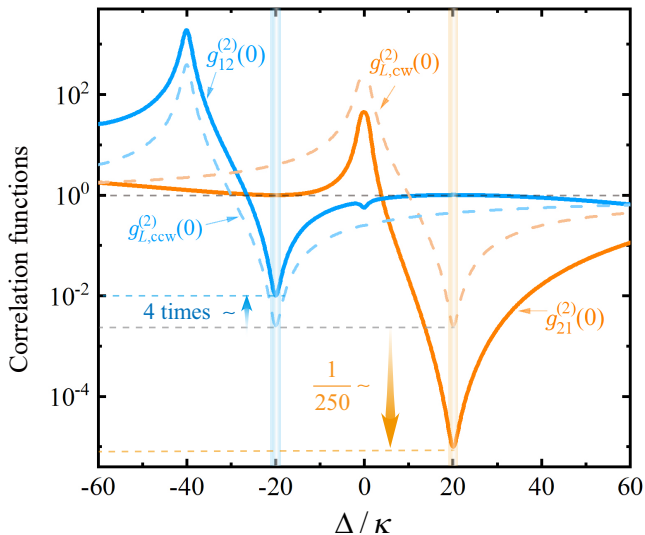


FIG. 3. The second-order correlation functions $g_{21}^{(2)}(0)$, $g_{12}^{(2)}(0)$, $g_{L,cw}^{(2)}(0)$, and $g_{L,ccw}^{(2)}(0)$ versus the detuning Δ/κ .

Based on the spatially separated transmission scheme discussed above, here we show that purely quantum nonreciprocity (nonreciprocal photon blockade) can be observed by considering the Kerr nonlinear interaction in one of the cavities (left cavity). We can predict that if a coherent field (weak driving field) is input from one of the ports, then we will observe photon blockade in the output field if the photons pass through the left cavity due to the strong Kerr nonlinear interaction, or we still obtain a coherent field in the output field if the photons pass through the right (linear) cavity.

The equal-time second-order correlation functions $g_{21}^{(2)}(0)$ and $g_{12}^{(2)}(0)$ are shown in Fig. 3. We achieve the nonreciprocal photon blockade in the parameter regions around the detuning $\Delta = \pm 20\kappa$ for high transmission rate $T_{21} = T_{12} \approx 1$. According to Figs. 2(a)-2(c), the photons transport from Port 1 to 2 passing through the left (nonlinear) cavity at $\Delta = 20\kappa$, thus we obtain sub-Poissonian statistical distribution ($g_{21}^{(2)}(0) \ll 1$) in the output field. In contrast, the photons transport from Port 2 to 1 passing through the right (linear) cavity at $\Delta = 20\kappa$, thus we obtain a Poisson statistical distribution ($g_{12}^{(2)}(0) \approx 1$) in the output field. On the contrary, at

$\Delta = -20\kappa$, the photons transport from Port 1 to 2 passing through the right cavity and we obtain a coherent output field ($g_{21}^{(2)}(0) \approx 1$); the photons transport from Port 2 to 1 passing through the left cavity and we obtain single photons ($g_{12}^{(2)}(0) \ll 1$) in the output field.

Surprisingly, the nonreciprocal photon blockade is enhanced nonreciprocally, i.e., the minimal value of $g_{21}^{(2)}(0)$ is much smaller than that of $g_{12}^{(2)}(0)$. For comparison, we also introduce the equal-time second-order correlation function of the photons in the left cavity as

$$g_{L,\sigma}^{(2)}(0) = \frac{\langle a_{L,\sigma}^\dagger a_{L,\sigma}^\dagger a_{L,\sigma} a_{L,\sigma} \rangle}{\langle a_{L,\sigma}^\dagger a_{L,\sigma} \rangle^2}, \quad (18)$$

where $\sigma = cw$ or ccw . To be clear, $g_{L,\sigma}^{(2)}(0)$ are also shown (dashed curves) in Fig. 3. The minimal value of $g_{12}^{(2)}(0)$ is about 4 times that of $g_{L,ccw}^{(2)}(0)$ and the minimal value of $g_{21}^{(2)}(0)$ is about 1/250 that of $g_{L,cw}^{(2)}(0)$. That means, in comparison with the photons in the (left) cavity, the photon blockade in the output fields is suppressed when the photons transport from Port 2 to 1, but significantly enhanced when the photons transport from Port 1 to 2. As the minimal values of $g_{L,cw}^{(2)}(0)$ and $g_{L,ccw}^{(2)}(0)$ are almost the same, thus we find that the minimal value of $g_{21}^{(2)}(0)$ is about three orders of magnitude smaller than that of $g_{12}^{(2)}(0)$. The mechanism for the photon blockade nonreciprocal enhancement is discussed in the next section.

V. MECHANISM FOR PHOTON BLOCKADE NONRECIPROCAL ENHANCEMENT

In order to understand the origin of photon blockade nonreciprocal enhancement predicted above, we derive the analytical expressions of the equal-time second-order correlation functions based on the Schrödinger equation.

The wave function of the system can be expanded on the Fock-state basis $|n_L n_R\rangle$, where n_L and n_R denote the number of photons in the left and right cavity, respectively. In the limit of weak driving field, the system can be truncated up to at most two photons, i.e., $n_L + n_R \leq 2$. In the truncated space, the state of the system can be described in the following form,

$$|\varphi(t)\rangle = C_{00}|00\rangle + C_{10}|10\rangle + C_{01}|01\rangle + C_{11}|11\rangle + C_{20}|20\rangle + C_{02}|02\rangle, \quad (19)$$

where $C_{n_L n_R}$ is the probability amplitude of the Fock state $|n_L n_R\rangle$. According to the quantum-trajectory method [98], the system (with decay rate 2κ for each cavity) is governed by a non-Hermitian Hamiltonian

$$\tilde{H}_\sigma = H_\sigma - i\kappa a_{L,\sigma}^\dagger a_{L,\sigma} - i\kappa a_{R,\sigma}^\dagger a_{R,\sigma}, \quad (20)$$

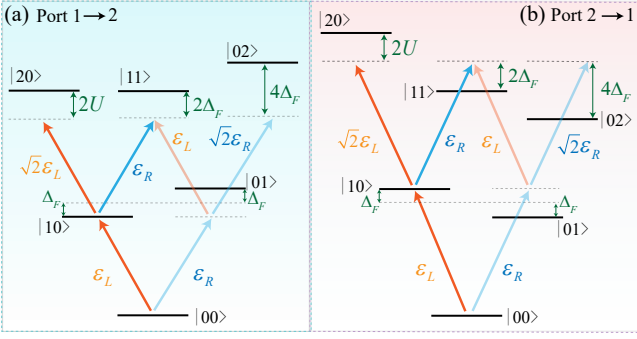


FIG. 4. Schematic energy spectrum of the system in the low-excitation subspace. (a) The photons transport from Port 1 to 2; (b) the photons transport from Port 2 to 1.

where $\sigma = \text{cw}$ or ccw . Substituting the wave function (19) and non-Hermitian Hamiltonian (20) into the Schrödinger equation $i\partial|\varphi(t)\rangle/\partial t = \tilde{H}_\sigma|\varphi(t)\rangle$, we can obtain the analytical expressions of the coefficients $C_{n_L n_R}$ in the steady state.

Based on the analytical expressions of the coefficients $C_{n_L n_R}$ in the steady state, the second-order correlation function of the field output from Port j (input from Port i) can be written as

$$g_{ji}^{(2)}(0) \approx \frac{2}{|C_{10}|^4} \left\{ |C_{20} - \sqrt{2}iC_{11}|^2 + |C_{02}|^2 - 2\text{Re} \left[(C_{20} - \sqrt{2}iC_{11}) C_{02}^* \right] \right\}, \quad (21)$$

where $ji = 21$ or 12 . Correspondingly, the second-order correlation function of the photons in the left cavity is given by

$$g_{L,\sigma}^{(2)}(0) \approx \frac{2|C_{20}|^2}{|C_{10}|^4} \quad (22)$$

with $\sigma = \text{cw}$ or ccw .

To find the optimal conditions for photon blockade nonreciprocal enhancement, we show the energy levels of the system in Fig. 4. According to the previous work [99], photon blockade should be observed under the conditions that the single-photon state is driven resonantly, i.e., resonant driving between levels $|00\rangle$ and $|10\rangle$, and the two-photon states are driven non-resonantly. Thus, we obtain one of the optimal conditions for photon blockade: $\Delta_{L,\text{cw}} = 0$ ($\Delta = \Delta_F$) for the photons transport from Port 1 to 2 [Fig. 4(a)]; $\Delta_{L,\text{ccw}} = 0$ ($\Delta = -\Delta_F$) for the photons transport from Port 2 to 1 [Fig. 4(b)]. Moreover, by comparing Eqs. (21) and (22), photon blockade enhancement should be observed under the conditions $|C_{2,0}| \approx \sqrt{2}|C_{1,1}| \gg |C_{0,2}|$, so that the term $(C_{20} - \sqrt{2}iC_{11})$ can be canceled out by destructive interference. The condition $|C_{2,0}| \approx \sqrt{2}|C_{1,1}|$ is achieved when the transition frequencies of $|10\rangle \rightarrow |20\rangle$ and $|10\rangle \rightarrow |11\rangle$ are the same, i.e., $U = \Delta_F$. Based on the above analysis, we find that the optimal conditions for photon blockade nonreciprocal

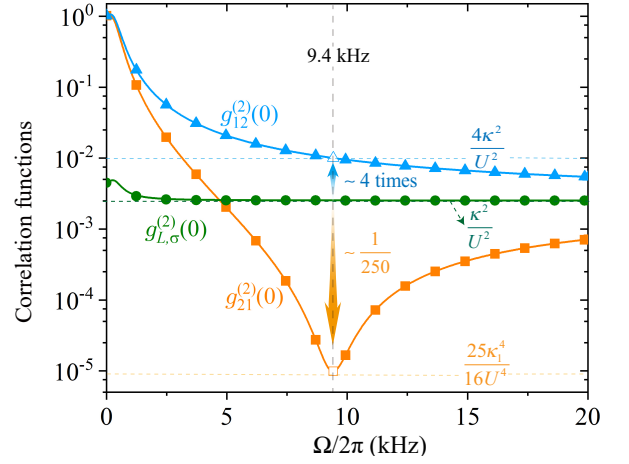


FIG. 5. The second-order correlation functions $g_{21}^{(2)}(0)$, $g_{12}^{(2)}(0)$, and $g_{L,\sigma}^{(2)}(0)$ versus the rotation frequency $\Omega/2\pi$. Here, $g_{21}^{(2)}(0)$ is plotted with the detuning $\Delta = \Delta_F$, $g_{21}^{(2)}(0)$ is plotted with the detuning $\Delta = -\Delta_F$.

enhancement are $\Delta = \Delta_F = U$, which are consistent well with the numerical results shown in Fig. 3.

To verify the optimal conditions ($\Delta = \Delta_F = U$) for photon blockade nonreciprocal enhancement, we show $g_{21}^{(2)}(0)$ and $g_{L,\text{cw}}^{(2)}(0)$ ($g_{12}^{(2)}(0)$ and $g_{L,\text{ccw}}^{(2)}(0)$), as functions of the rotation frequency $\Omega/2\pi$, under the resonant condition $\Delta = \Delta_F$ ($\Delta = -\Delta_F$), in Fig. 5. When the two cavities are not spinning or spinning with a low angular velocity $\Omega/2\pi < 5$ kHz, we have $g_{12}^{(2)}(0) > g_{21}^{(2)}(0) > g_{L,\text{cw}}^{(2)}(0) = g_{L,\text{ccw}}^{(2)}(0)$. But with the increase of the angular velocity Ω , $g_{21}^{(2)}(0)$ decreases rapidly and the system comes into the regime of photon blockade nonreciprocal enhancement, i.e., $g_{12}^{(2)}(0) > g_{L,\text{cw}}^{(2)}(0) = g_{L,\text{ccw}}^{(2)}(0) > g_{21}^{(2)}(0)$. Most notably, $g_{21}^{(2)}(0)$ reaches its minimal value at the angular velocity $\Omega/2\pi \approx 9.4$ kHz, i.e., $\Delta_F \approx U$, and it is about three orders of magnitude smaller than that of $g_{12}^{(2)}(0)$. This indicates a purely nonreciprocal photon blockade with direction-dependent enhancement in the spinning cavities, and such effect has not been revealed previously.

Now, we focus on the optimal conditions for photon blockade nonreciprocal enhancement, i.e., $\Delta_{L,\text{cw}} = 0$ ($\Delta = \Delta_F = U$) for the photons transport from Port 1 to 2 and $\Delta_{L,\text{ccw}} = 0$ ($\Delta = -\Delta_F = -U$) for the photons transport from Port 2 to 1. Under these conditions, the probability amplitudes for two-photon states in the steady state are approximately given by

$$C_{20} \approx \frac{-\varepsilon_L^2 [(2U^2 - \kappa^2) i \pm 4U\kappa]}{2\sqrt{2}U^3\kappa}, \quad (23)$$

$$C_{11} \approx \frac{\varepsilon_L^2 [iU\kappa + (\kappa^2 \mp 2U^2)]}{4U^3\kappa}, \quad (24)$$

$$C_{02} \approx \frac{-\varepsilon_L^2}{4\sqrt{2}U^2}, \quad (25)$$

where, the plus sign (+) in Eq. (23) and the minus sign (−) in Eq. (24) denote the case that the photons transport from Port 1 to 2, and the minus sign (−) in Eq. (23) and the plus sign (+) in Eq. (24) denote the case that the photons transport from Port 2 to 1. In the strong nonlinear regime ($U \gg \kappa$), we have $C_{20} \approx \sqrt{2}iC_{11}$ for photons transport from Port 1 to 2, and they are canceled out by destructive interference, with $C_{20} - \sqrt{2}iC_{11} \approx 0$. Meanwhile, we have $C_{20} \approx -\sqrt{2}iC_{11}$ for photons transport from Port 2 to 1, and there is constructive interference between them, with $C_{20} - \sqrt{2}iC_{11} \approx 2C_{20}$. Based on the approximate expressions of the probability amplitudes, the second-order correlation functions are obtained analytically as

$$g_{21}^{(2)}(0) \approx \frac{25\kappa^4}{16U^4}, \quad (26)$$

$$g_{12}^{(2)}(0) \approx 4\frac{\kappa^2}{U^2}, \quad (27)$$

$$g_{L,\sigma}^{(2)}(0) \approx \frac{\kappa^2}{U^2}. \quad (28)$$

The analytical expressions of $g_{12}^{(2)}(0)$, $g_{21}^{(2)}(0)$, and $g_{L,\sigma}^{(2)}(0)$ [Eqs. (27)-(28)] are shown (dashed lines) in Fig. 5. It is clear that we have $g_{12}^{(2)}(0) \approx 4g_{L,\sigma}^{(2)}(0)$ and $g_{21}^{(2)}(0) \approx g_{L,\sigma}^{(2)}(0)/256$, which are consistent well with the numerical results in Figs. 3 and 5. It is worth mentioning that we have $g_{21}^{(2)}(0) \propto (\kappa/U)^4$ and $g_{L,\sigma}^{(2)}(0) \propto (\kappa/U)^2$, i.e., the spinning cavities can be used to achieve scaling enhancement of photon blockade [100].

VI. CONCLUSION

In conclusion, we have proposed a spatially separated transmission scheme that the photons transport in differ-

ent directions take different paths, in an optical system consisting of two spinning cavities coupled indirectly by two common drop-filter waveguides. Based on the spatially separated transmission scheme, we demonstrated a purely quantum nonreciprocity (nonreciprocal photon blockade) by considering the Kerr nonlinear interaction in one of the cavities (left cavity). Even more interestingly, the nonreciprocal photon blockade is enhanced nonreciprocally, i.e., the nonreciprocal photon blockade is enhanced when the photons transport in one direction but suppressed in the reverse direction. We have identified that the nonreciprocal enhancement of the photon blockade is induced by the destructive or constructive interference between two paths for two photons passing through the whole system. The spinning cavities may also work when they contain other nonlinear interactions, such as second-order nonlinearity [69–71], optomechanical interaction [72–74], or atom-cavity interaction [75–79], to achieve more quantum nonreciprocal effects, e.g., nonreciprocal entanglement [59–62] and nonreciprocal squeezing [63–66]. Moreover, the spatially separated transmission scheme may also be extended to study other nonreciprocal effects, such as nonreciprocal cooling [101–103], nonreciprocal lasing [104–108], and nonreciprocal (topology) energy band by considering a array of cavities [109–112].

ACKNOWLEDGMENTS

This work is supported by the National Natural Science Foundation of China (Grants No. 12064010 and No. 12247105), the science and technology innovation Program of Hunan Province (Grant No. 2022RC1203), and Hunan provincial major sci-tech program (Grant No. 2023ZJ1010).

-
- [1] D. Jalas, A. Petrov, M. Eich, W. Freude, S. Fan, Z. Yu, R. Baets, M. Popović, A. Melloni, J. D. Joannopoulos, M. Vanwolleghem, C. R. Doerr, and H. Renner, What is – and what is not – an optical isolator, *Nature Photon.* **7**, 579 (2013).
 - [2] C. Sayrin, C. Junge, R. Mitsch, B. Albrecht, D. O’Shea, P. Schneeweiss, J. Volz, and A. Rauschenbeutel, Nanophotonic Optical Isolator Controlled by the Internal State of Cold Atoms, *Phys. Rev. X* **5**, 041036 (2015).
 - [3] X.-W. Xu, L. N. Song, Q. Zheng, Z. H. Wang, and Y. Li, Optomechanically induced nonreciprocity in a three-mode optomechanical system, *Phys. Rev. A* **98**, 063845 (2018).
 - [4] L. Tang, J. Tang, W. Zhang, G. Lu, H. Zhang, Y. Zhang, K. Xia, and M. Xiao, On-chip chiral single-photon interface: Isolation and unidirectional emission, *Phys. Rev. A* **99**, 043833 (2019).
 - [5] L. Tang, J. Tang, M. Chen, F. Nori, M. Xiao, and K. Xia, Quantum squeezing induced optical nonreciprocity, *Phys. Rev. Lett.* **128**, 083604 (2022).
 - [6] W. Nie, L. Wang, Y. Wu, A. Chen, and Y. Lan, Optomechanical ratchet resonators, *Sci. China Phys. Mech. Astron.* **65**, 230311 (2022).
 - [7] X.-W. Xu and Y. Li, Optical nonreciprocity and optomechanical circulator in three-mode optomechanical systems, *Phys. Rev. A* **91**, 053854 (2015).
 - [8] F. Ruesink, J. P. Mathew, M.-A. Miri, A. Alù, and E. Verhagen, Optical circulation in a multimode optomechanical resonator, *Nat. Commun.* **9**, 1798 (2018).
 - [9] K. Xia, F. Nori, and M. Xiao, Cavity-free optical isolators and circulators using a chiral cross-kerr nonlinearity, *Phys. Rev. Lett.* **121**, 203602 (2018).
 - [10] E.-Z. Li, D.-S. Ding, Y.-C. Yu, M.-X. Dong, L. Zeng, W.-H. Zhang, Y.-H. Ye, H.-Z. Wu, Z.-H. Zhu, W. Gao, G.-C. Guo, and B.-S. Shi, Experimental demonstration of cavity-free optical isolators and optical circulators, *Phys. Rev. Res.* **2**, 033517 (2020).

- [11] W. Yan, Y. Yang, S. Liu, Y. Zhang, S. Xia, T. Kang, W. Yang, J. Qin, L. Deng, and L. Bi, Waveguide-integrated high-performance magneto-optical isolators and circulators on silicon nitride platforms, *Optica* **7**, 1555 (2020).
- [12] A. Metelmann and A. A. Clerk, Nonreciprocal photon transmission and amplification via reservoir engineering, *Phys. Rev. X* **5**, 021025 (2015).
- [13] Y. Li, Y. Y. Huang, X. Z. Zhang, and L. Tian, Optical directional amplification in a three-mode optomechanical system, *Opt. Express* **25**, 18907 (2017).
- [14] D. Malz, L. D. Tóth, N. R. Bernier, A. K. Feofanov, T. J. Kippenberg, and A. Nunnenkamp, Quantum-limited directional amplifiers with optomechanics, *Phys. Rev. Lett.* **120**, 023601 (2018).
- [15] Z. Shen, Y. L. Zhang, Y. Chen, F. W. Sun, X. B. Zou, G. C. Guo, C. L. Zou, and C. H. Dong, Reconfigurable optomechanical circulator and directional amplifier, *Nat. Commun.* **9**, 1797 (2018).
- [16] L. N. Song, Q. Zheng, X.-W. Xu, C. Jiang, and Y. Li, Optimal unidirectional amplification induced by optical gain in optomechanical systems, *Phys. Rev. A* **100**, 043835 (2019).
- [17] C. Jiang, L. N. Song, and Y. Li, Directional phase-sensitive amplifier between microwave and optical photons, *Phys. Rev. A* **99**, 023823 (2019).
- [18] X. Z. Zhang, L. Tian, and Y. Li, Optomechanical transistor with mechanical gain, *Phys. Rev. A* **97**, 043818 (2018).
- [19] L. Mercier de Lépinay, E. Damskågg, C. F. Ockeloen-Korppi, and M. A. Sillanpää, Realization of directional amplification in a microwave optomechanical device, *Phys. Rev. Appl.* **11**, 034027 (2019).
- [20] L. Mercier de Lépinay, C. F. Ockeloen-Korppi, D. Malz, and M. A. Sillanpää, Nonreciprocal transport based on cavity floquet modes in optomechanics, *Phys. Rev. Lett.* **125**, 023603 (2020).
- [21] X.-W. Xu, Y. Li, A.-X. Chen, and Y.-x. Liu, Nonreciprocal conversion between microwave and optical photons in electro-optomechanical systems, *Phys. Rev. A* **93**, 023827 (2016).
- [22] X.-W. Xu, A.-X. Chen, Y. Li, and Y.-x. Liu, Nonreciprocal single-photon frequency converter via multiple semi-infinite coupled-resonator waveguides, *Phys. Rev. A* **96**, 053853 (2017).
- [23] G. A. Peterson, F. Lecocq, K. Cicak, R. W. Simmonds, J. Aumentado, and J. D. Teufel, Demonstration of Efficient Nonreciprocity in a Microwave Optomechanical Circuit, *Phys. Rev. X* **7**, 031001 (2017).
- [24] N. R. Bernier, L. D. Tóth, A. Koottandavida, M. A. Ioannou, D. Malz, A. Nunnenkamp, A. K. Feofanov, and T. J. Kippenberg, Nonreciprocal reconfigurable microwave optomechanical circuit, *Nat. Commun.* **8**, 604 (2017).
- [25] S. Barzanjeh, M. Wulf, M. Peruzzo, M. Kalaei, P. B. Dieterle, O. Painter, and J. M. Fink, Mechanical on-chip microwave circulator, *Nat. Commun.* **8**, 953 (2017).
- [26] G. Li, X. Xiao, Y. Li, and X. Wang, Tunable optical nonreciprocity and a phonon-photon router in an optomechanical system with coupled mechanical and optical modes, *Phys. Rev. A* **97**, 023801 (2018).
- [27] L. Du, Y.-T. Chen, and Y. Li, Nonreciprocal frequency conversion with chiral Λ -type atoms, *Phys. Rev. Res.* **3**, 043226 (2021).
- [28] D. L. Sounas and A. Alù, Non-reciprocal photonics based on time modulation, *Nature Photon.* **11**, 774 (2017).
- [29] L. Bi, J. Hu, P. Jiang, D. H. Kim, G. F. Dionne, L. C. Kimerling, and C. A. Ross, On-chip optical isolation in monolithically integrated non-reciprocal optical resonators, *Nature Photon.* **5**, 758 (2011).
- [30] M. Shalaby, M. Peccianti, Y. Ozturk, and R. Morandotti, A magnetic non-reciprocal isolator for broadband terahertz operation, *Nat. Commun.* **4**, 1558 (2013).
- [31] Y. Shoji and T. Mizumoto, Magneto-optical non-reciprocal devices in silicon photonics, *Sci. Technol. Adv. Mater.* **15**, 014602 (2014).
- [32] L. Fan, J. Wang, L. T. Varghese, H. Shen, B. Niu, Y. Xuan, A. M. Weiner, and M. Qi, An All-Silicon Passive Optical Diode, *Science* **335**, 447 (2012).
- [33] D. L. Sounas, J. Soric, and A. Alu, Broadband passive isolators based on coupled nonlinear resonances, *Nat. Electron.* **1**, 113 (2018).
- [34] P. Yang, X. Xia, H. He, S. Li, X. Han, P. Zhang, G. Li, P. Zhang, J. Xu, Y. Yang, and T. Zhang, Realization of nonlinear optical nonreciprocity on a few-photon level based on atoms strongly coupled to an asymmetric cavity, *Phys. Rev. Lett.* **123**, 233604 (2019).
- [35] K. Fang, Z. Yu, and S. Fan, Realizing effective magnetic field for photons by controlling the phase of dynamic modulation, *Nature Photon.* **6**, 782 (2012).
- [36] L. D. Tzuang, K. Fang, P. Nussenzeig, S. Fan, and M. Lipson, Non-reciprocal phase shift induced by an effective magnetic flux for light, *Nature Photon.* **8**, 701 (2014).
- [37] K. Fang, J. Luo, A. Metelmann, M. H. Matheny, F. Marquardt, A. A. Clerk, and O. Painter, Generalized nonreciprocity in an optomechanical circuit via synthetic magnetism and reservoir engineering, *Nature Phys.* **13**, 465 (2017).
- [38] X. Lu, W. Cao, W. Yi, H. Shen, and Y. Xiao, Nonreciprocity and quantum correlations of light transport in hot atoms via reservoir engineering, *Phys. Rev. Lett.* **126**, 223603 (2021).
- [39] Z. Yu and S. Fan, Complete optical isolation created by indirect interband photonic transitions, *Nature Photon.* **3**, 91 (2009).
- [40] H. Lira, Z. Yu, S. Fan, and M. Lipson, Electrically driven nonreciprocity induced by interband photonic transition on a silicon chip, *Phys. Rev. Lett.* **109**, 033901 (2012).
- [41] M. Castellanos Muñoz, A. Y. Petrov, L. O'Faolain, J. Li, T. F. Krauss, and M. Eich, Optically induced indirect photonic transitions in a slow light photonic crystal waveguide, *Phys. Rev. Lett.* **112**, 053904 (2014).
- [42] H. Tian, J. Liu, A. Siddharth, R. N. Wang, T. Blésin, J. He, T. J. Kippenberg, and S. A. Bhave, Magnetic-free silicon nitride integrated optical isolator, *Nature Photon.* **15**, 828 (2021).
- [43] C. E. Rüter, K. G. Makris, R. El-Ganainy, D. N. Christodoulides, M. Segev, and D. Kip, Observation of parity-time symmetry in optics, *Nature Phys.* **6**, 192 (2010).
- [44] B. Peng, Ş. K. Özdemir, F. Lei, F. Monifi, M. Gianfreda, G. L. Long, S. Fan, F. Nori, C. M. Bender, and L. Yang, Parity-time-symmetric whispering-gallery microcavities, *Nature Phys.* **10**, 394 (2014).

- [45] L. Chang, X. Jiang, S. Hua, C. Yang, J. Wen, L. Jiang, G. Li, G. Wang, and M. Xiao, Parity-time symmetry and variable optical isolation in active-passive-coupled microresonators, *Nature Photon.* **8**, 524 (2014).
- [46] H. Ramezani, H.-K. Li, Y. Wang, and X. Zhang, Unidirectional spectral singularities, *Phys. Rev. Lett.* **113**, 263905 (2014).
- [47] D.-W. Wang, H.-T. Zhou, M.-J. Guo, J.-X. Zhang, J. Evers, and S.-Y. Zhu, Optical diode made from a moving photonic crystal, *Phys. Rev. Lett.* **110**, 093901 (2013).
- [48] S. A. R. Horsley, J.-H. Wu, M. Artoni, and G. C. La Rocca, Optical nonreciprocity of cold atom bragg mirrors in motion, *Phys. Rev. Lett.* **110**, 223602 (2013).
- [49] S. Zhang, Y. Hu, G. Lin, Y. Niu, K. Xia, J. Gong, and S. Gong, Thermal-motion-induced non-reciprocal quantum optical system, *Nature Photon.* **12**, 744 (2018).
- [50] S. Maayani, R. Dahan, Y. Kligerman, E. Moses, A. U. Hassan, H. Jing, F. Nori, D. N. Christodoulides, and T. Carmon, Flying couplers above spinning resonators generate irreversible refraction, *Nature (London)* **558**, 569 (2018).
- [51] M. Scheucher, A. Hilico, E. Will, J. Volz, and A. Rauschenbeutel, Quantum optical circulator controlled by a single chirally coupled atom, *Science* **354**, 1577 (2016).
- [52] P. Lodahl, S. Mahmoodian, S. Stobbe, A. Rauschenbeutel, P. Schneeweiss, J. Volz, H. Pichler, and P. Zoller, Chiral quantum optics, *Nature (London)* **541**, 473 (2017).
- [53] J.-S. Tang, W. Nie, L. Tang, M. Chen, X. Su, Y. Lu, F. Nori, and K. Xia, Nonreciprocal single-photon band structure, *Phys. Rev. Lett.* **128**, 203602 (2022).
- [54] R. Huang, A. Miranowicz, J.-Q. Liao, F. Nori, and H. Jing, Nonreciprocal photon blockade, *Phys. Rev. Lett.* **121**, 153601 (2018).
- [55] X. Xu, Y. Zhao, H. Wang, H. Jing, and A. Chen, Quantum nonreciprocity in quadratic optomechanics, *Photon. Res.* **8**, 143 (2020).
- [56] X. Xia, X. Zhang, J. Xu, H. Li, Z. Fu, and Y. Yang, Giant nonreciprocal unconventional photon blockade with a single atom in an asymmetric cavity, *Phys. Rev. A* **104**, 063713 (2021).
- [57] H. Xie, L.-W. He, X. Shang, G.-W. Lin, and X.-M. Lin, Nonreciprocal photon blockade in cavity optomagnonics, *Phys. Rev. A* **106**, 053707 (2022).
- [58] C.-P. Shen, J.-Q. Chen, X.-F. Pan, Y.-M. Ren, X.-L. Dong, X.-L. Hei, Y.-F. Qiao, and P.-B. Li, Tunable nonreciprocal photon correlations induced by directional quantum squeezing, *Phys. Rev. A* **108**, 023716 (2023).
- [59] Y.-F. Jiao, S.-D. Zhang, Y.-L. Zhang, A. Miranowicz, L.-M. Kuang, and H. Jing, Nonreciprocal optomechanical entanglement against backscattering losses, *Phys. Rev. Lett.* **125**, 143605 (2020).
- [60] Y.-F. Jiao, J.-X. Liu, Y. Li, R. Yang, L.-M. Kuang, and H. Jing, Nonreciprocal enhancement of remote entanglement between nonidentical mechanical oscillators, *Phys. Rev. Appl.* **18**, 064008 (2022).
- [61] Y.-L. Ren, Nonreciprocal optical-microwave entanglement in a spinning magnetic resonator, *Opt. Lett.* **47**, 1125 (2022).
- [62] J. Chen, X.-G. Fan, W. Xiong, D. Wang, and L. Ye, Nonreciprocal entanglement in cavity-magnon optomechanics, *Phys. Rev. B* **108**, 024105 (2023).
- [63] S.-S. Chen, S.-S. Meng, H. Deng, and G.-J. Yang, Nonreciprocal mechanical squeezing in a spinning optomechanical system, *Ann. Phys. (Berlin)* **533**, 2000343 (2021).
- [64] B. Zhao, K.-X. Zhou, M.-R. Wei, J. Cao, and Q. Guo, Nonreciprocal strong mechanical squeezing based on the sagnac effect and two-tone driving, *Opt. Lett.* **49**, 486 (2024).
- [65] Q. Guo, K.-X. Zhou, C.-H. Bai, Y. Zhang, G. Li, and T. Zhang, Nonreciprocal mechanical squeezing in a spinning cavity optomechanical system via pump modulation, *Phys. Rev. A* **108**, 033515 (2023).
- [66] J. Wang, Q. Zhang, Y.-F. Jiao, S.-D. Zhang, T.-X. Lu, Z. Li, C.-W. Qiu, and H. Jing, Quantum advantage of one-way squeezing in enhancing weak-force sensing, [arXiv:2403.09979](https://arxiv.org/abs/2403.09979).
- [67] P. Yang, M. Li, X. Han, H. He, G. Li, C.-L. Zou, P. Zhang, Y. Qian, and T. Zhang, Non-reciprocal cavity polariton with atoms strongly coupled to optical cavity, *Laser Photonics Rev.* **17**, 2200574 (2023).
- [68] Y.-W. Jing, Quantum spinning photonic circulator, *Sci. Rep.* **12**, 5844 (2022).
- [69] K. Wang, Q. Wu, Y.-F. Yu, and Z.-M. Zhang, Nonreciprocal photon blockade in a two-mode cavity with a second-order nonlinearity, *Phys. Rev. A* **100**, 053832 (2019).
- [70] H. Z. Shen, Q. Wang, J. Wang, and X. X. Yi, Nonreciprocal unconventional photon blockade in a driven dissipative cavity with parametric amplification, *Phys. Rev. A* **101**, 013826 (2020).
- [71] C. Gou and X. Hu, Simultaneous nonreciprocal photon blockade in two coupled spinning resonators via sagnac-fizeau shift and parametric amplification, *Phys. Rev. A* **108**, 043723 (2023).
- [72] B. Li, R. Huang, X. Xu, A. Miranowicz, and H. Jing, Nonreciprocal unconventional photon blockade in a spinning optomechanical system, *Photon. Res.* **7**, 630 (2019).
- [73] Y.-M. Liu, J. Cheng, H.-F. Wang, and X. Yi, Nonreciprocal photon blockade in a spinning optomechanical system with nonreciprocal coupling, *Opt. Express* **31**, 12847 (2023).
- [74] X. Shang, H. Xie, and X.-M. Lin, Nonreciprocal photon blockade in a spinning optomechanical resonator, *Laser Phys. Lett.* **18**, 115202 (2021).
- [75] W. S. Xue, H. Z. Shen, and X. X. Yi, Nonreciprocal conventional photon blockade in driven dissipative atom-cavity, *Opt. Lett.* **45**, 4424 (2020).
- [76] Y.-W. Jing, H.-Q. Shi, and X.-W. Xu, Nonreciprocal photon blockade and directional amplification in a spinning resonator coupled to a two-level atom, *Phys. Rev. A* **104**, 033707 (2021).
- [77] J. Wang, Q. Wang, and H. Z. Shen, Nonreciprocal unconventional photon blockade with spinning atom-cavity, *EPL* **134**, 64003 (2021).
- [78] Y.-M. Liu, J. Cheng, H.-F. Wang, and X. Yi, Simultaneous nonreciprocal conventional photon blockades of two independent optical modes by a two-level system, *Phys. Rev. A* **107**, 063701 (2023).
- [79] W. Zhang, T. Wang, S. Liu, S. Zhang, and H.-F. Wang, Nonreciprocal photon blockade in a spinning resonator coupled to two two-level atoms, *Sci. China Phys. Mech. Astron.* **66**, 240313 (2023).

- [80] X.-W. Xu, Y. Li, B. Li, H. Jing, and A.-X. Chen, Nonreciprocity via nonlinearity and synthetic magnetism, *Phys. Rev. Appl.* **13**, 044070 (2020).
- [81] A. Graf, S. D. Rogers, J. Staffa, U. A. Javid, D. H. Griffith, and Q. Lin, Nonreciprocity in photon pair correlations of classically reciprocal systems, *Phys. Rev. Lett.* **128**, 213605 (2022).
- [82] Y. Xiang, Y. Zuo, X.-W. Xu, R. Huang, and H. Jing, Switching classical and quantum nonreciprocities with a single spinning resonator, *Phys. Rev. A* **108**, 043702 (2023).
- [83] G. B. Malykin, The sagnac effect: correct and incorrect explanations, *Phys.-Usp.* **43**, 1229 (2000).
- [84] P. Marin-Palomo, J. N. Kemal, M. Karpov, A. Korodts, J. Pfeifle, M. H. P. Pfeiffer, P. Trocha, S. Wolf, V. Brasch, M. H. Anderson, R. Rosenberger, K. Vijayan, W. Freude, T. J. Kippenberg, and C. Koos, Microresonator-based solitons for massively parallel coherent optical communications, *Nature (London)* **546**, 274 (2017).
- [85] Z.-H. Peng, C.-X. Jia, Y.-Q. Zhang, J.-B. Yuan, and L.-M. Kuang, Level attraction and \mathcal{PT} symmetry in indirectly coupled microresonators, *Phys. Rev. A* **102**, 043527 (2020).
- [86] C. W. Gardiner and M. J. Collett, Input and output in damped quantum systems: Quantum stochastic differential equations and the master equation, *Phys. Rev. A* **31**, 3761 (1985).
- [87] H. Carmichael, *An Open Systems Approach to Quantum Optics* (Springer Berlin Heidelberg, Berlin, Heidelberg, 1993).
- [88] V. Huet, A. Rasoloniaina, P. Guillemé, P. Rochard, P. Féron, M. Mortier, A. Levenson, K. Bencheikh, A. Yacomotti, and Y. Dumeige, Millisecond Photon Lifetime in a Slow-Light Microcavity, *Phys. Rev. Lett.* **116**, 133902 (2016).
- [89] N. G. Pavlov, G. Lihachev, S. Koptyaev, E. Lucas, M. Karpov, N. M. Kondratiev, I. A. Bilenko, T. J. Kippenberg, and M. L. Gorodetsky, Soliton dual frequency combs in crystalline microresonators, *Opt. Lett.* **42**, 514 (2017).
- [90] G. C. Righini, Y. Dumeige, P. Féron, M. Ferrari, G. Nunzi Conti, D. Ristic, and S. Soria, Whispering gallery mode microresonators: fundamentals and applications, *La Rivista del Nuovo Cimento* **34**, 435 (2011).
- [91] I. Schuster, A. Kubanek, A. Fuhrmanek, T. Puppe, P. W. H. Pinkse, K. Murr, and G. Rempe, Nonlinear spectroscopy of photons bound to one atom, *Nature Phys.* **4**, 382 (2008).
- [92] Z. Shen, C.-H. Dong, Y. Chen, Y.-F. Xiao, F.-W. Sun, and G.-C. Guo, Compensation of the Kerr effect for transient optomechanically induced transparency in a silica microsphere, *Opt. Lett.* **41**, 1249 (2016).
- [93] S. M. Spillane, T. J. Kippenberg, K. J. Vahala, K. W. Goh, E. Wilcut, and H. J. Kimble, Ultrahigh-Q toroidal microresonators for cavity quantum electrodynamics, *Phys. Rev. A* **71**, 013817 (2005).
- [94] K. J. Vahala, Optical microcavities, *Nature (London)* **424**, 839 (2003).
- [95] J. A. Zielinska and M. W. Mitchell, Self-tuning optical resonator, *Opt. Lett.* **42**, 5298 (2017).
- [96] J. Ahn, Z. Xu, J. Bang, Y.-H. Deng, T. M. Hoang, Q. Han, R.-M. Ma, and T. Li, Optically Levitated Nanodumbbell Torsion Balance and GHz Nanomechanical Rotor, *Phys. Rev. Lett.* **121**, 033603 (2018).
- [97] Y. Jin, J. Yan, S. J. Rahman, J. Li, X. Yu, and J. Zhang, 6 GHz hyperfast rotation of an optically levitated nanoparticle in vacuum, *Photon. Res.* **9**, 1344 (2021).
- [98] M. B. Plenio and P. L. Knight, The quantum-jump approach to dissipative dynamics in quantum optics, *Rev. Mod. Phys.* **70**, 101 (1998).
- [99] A. Imamoglu, H. Schmidt, G. Woods, and M. Deutsch, Strongly interacting photons in a nonlinear cavity, *Phys. Rev. Lett.* **79**, 1467 (1997).
- [100] Z.-H. Liu and X.-W. Xu, Scaling enhancement of photon blockade in output fields, [arXiv:2403.18299 \[quant-ph\]](https://arxiv.org/abs/2403.18299).
- [101] S. J. M. Habraken, K. Stannigel, M. D. Lukin, P. Zoller, and P. Rabl, Continuous mode cooling and phonon routers for phononic quantum networks, *New J. Phys.* **14**, 115004 (2012).
- [102] H. Xu, L. Jiang, A. A. Clerk, and J. G. E. Harris, Nonreciprocal control and cooling of phonon modes in an optomechanical system, *Nature (London)* **568**, 65 (2019).
- [103] D.-G. Lai, J.-F. Huang, X.-L. Yin, B.-P. Hou, W. Li, D. Vitali, F. Nori, and J.-Q. Liao, Nonreciprocal ground-state cooling of multiple mechanical resonators, *Phys. Rev. A* **102**, 011502 (2020).
- [104] Y. Jiang, S. Maayani, T. Carmon, F. Nori, and H. Jing, Nonreciprocal phonon laser, *Phys. Rev. Appl.* **10**, 064037 (2018).
- [105] A. Muñoz de las Heras and I. Carusotto, Unidirectional lasing in nonlinear taiji microring resonators, *Phys. Rev. A* **104**, 043501 (2021).
- [106] Y. Xu, J.-Y. Liu, W. Liu, and Y.-F. Xiao, Nonreciprocal phonon laser in a spinning microwave magnomechanical system, *Phys. Rev. A* **103**, 053501 (2021).
- [107] Y.-J. Xu and J. Song, Nonreciprocal magnon laser, *Opt. Lett.* **46**, 5276 (2021).
- [108] T.-X. Lu, Y. Wang, K. Xia, X. Xiao, L.-M. Kuang, and H. Jing, Quantum squeezing induced nonreciprocal phonon laser, *Sci. China Phys. Mech. Astron.* **67**, 260312 (2024).
- [109] B. Bahari, A. Ndao, F. Vallini, A. El Amili, Y. Fainman, and B. Kanté, Nonreciprocal lasing in topological cavities of arbitrary geometries, *Science* **358**, 636 (2017).
- [110] A. Seif, W. DeGottardi, K. Esfarjani, and M. Hafezi, Thermal management and non-reciprocal control of phonon flow via optomechanics, *Nat. Commun.* **9**, 1207 (2018).
- [111] N. Hu, Z.-X. Tang, and X.-W. Xu, Broadband optical nonreciprocity via nonreciprocal band structure, *Phys. Rev. A* **108**, 063516 (2023).
- [112] H. Qin, Z. Zhang, Q. Chen, and R. Fleury, Disclination states in nonreciprocal topological networks, *Phys. Rev. Res.* **6**, 013031 (2024).